

Enhancement and Quenching Regimes in Metal–Semiconductor Hybrid Optical Nanosources

Pierre Viste, Jérôme Plain,* Rodolphe Jaffiol, Alexandre Vial, Pierre Michel Adam, and Pascal Royer

Laboratoire de Nanotechnologie et d'Instrumentation Optique, ICD CNRS FRE 2848, Université de Technologie de Troyes BP 2060 Troyes cedex, France

One of the work-horses of nano-optics is the realization of intense and stable light sources, confined at the nanoscale. To design nanoscale light sources, different strategies have been developed. Metal nanoparticles in particular, have the ability to localize and strongly enhance the incident electromagnetic field when excited at their plasmon resonance.^{1,2} This property has been experimentally demonstrated and widely used for numerous applications such as near field photopolymerization,³ surface enhanced Raman scattering,⁴ or metal enhanced fluorescence.⁵ Another route is to use hybrid systems composed by a metal nanostructure and fluorophores to increase the luminescence yield of the resulting hybrid system.⁵ An alternative hybrid source is the spaser approach proposed by Bergman and Stockman.⁶ The principle is based on the energy transfer from a fluorophore to the plasmon state of a metal nanostructure which induces a stimulated emission of the amplified plasmon state, as in laser.^{7,8} Generally, the interplay between metal nanoparticle and luminescent species involves two major phenomena:^{9–12} the first one is an enhancement of the local excitation field, and the second one is the modification of the radiative and nonradiative decay rates of the fluorophores, inducing a change of fluorescence lifetime and quantum yield.¹³ The competition between these processes results in two opposite observations as reported in the literature: quenching of luminescence or on the contrary its enhancement.^{10,11,14–16} Different parameters play a determinant role in the quenching and enhancement mechanisms but their influence is still debated. Particularly, the spectral position and the influence of

ABSTRACT We report on the emission of hybrid nanosources composed of gold nanoparticles coupled with quantum dots. The emission relies on energy transfer from the quantum dots to gold nanoparticles which could be de-excited through radiative plasmon relaxation. The dependence of the emission efficiency is studied systematically as a function of the size of gold nanoparticles and interdistance between gold nanoparticles and quantum dots. We demonstrate a size-dependent transition between quenching and enhancement and a nonradiative energy transfer from the quantum dots to the gold nanoparticles.

KEYWORDS: gold nanoparticles · fluorescence enhancement · fluorescence quenching · quantum dots · energy transfer

the localized surface plasmon resonance (LSPR) compared to the absorption and emission maximum of luminescent species is determinant.^{11,12,15–20}

In this paper, we report on a systematic study of the coupling between gold nanoparticles and quantum dots. First, we study the influence of the spectral position LSPR with respect to the emission wavelength of quantum dots (QDs). Second, we report on the influence of the coupling between the QDs and the gold nanoparticles (GNPs) by varying their interdistance. We show that there is a nonradiative transfer of energy from the QDs to the GNP, leading to photon emission if the transferred energy is resonant with the plasmon state of the LSPR.

RESULTS AND DISCUSSION

The extinction spectra of GNP with different diameters before (respectively, after) deposition of the quantum-dot-doped thin film are shown in Figure 1. By changing the diameter from 80 to 160 nm, the LSPR wavelength varies from 580 nm (respectively, 618 nm) to 700 nm (respectively, 732 nm). For each array, the extinction spectrum is adjusted using a Lorentzian function to determine the maximum. Note that the single apparent mode is the dipolar one.

*Address correspondence to jerome.plain@utt.fr.

Received for review September 25, 2009 and accepted December 30, 2009.

Published online January 5, 2010.
10.1021/nn901294d

© 2010 American Chemical Society

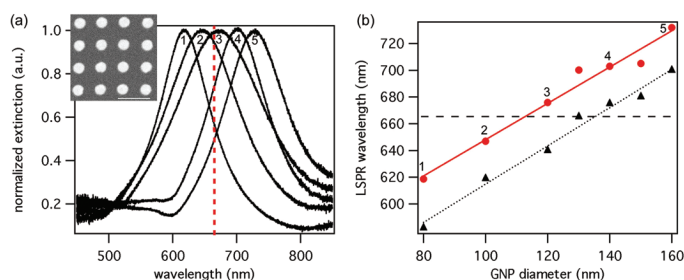


Figure 1. (a) Extinction spectrum of GNP with diameter (1) 80, (2) 100, (3) 120, (4) 140, (5) 160 nm, respectively. Inset shows SEM micrograph of typical GNP array. White bar represents 500 nm. (b) LSPR wavelength as a function of the gold nanoparticle diameter measured (triangle) in air and (circle) in PMMA-QD. Lines are guides for the eye.

Figure 1b shows the LSPR peak maximum as a function of GNP size. Note that the extinction spectrum maximum, corresponding to the localized surface plasmon resonance, red-shifts with increasing diameter. This redshift is commonly observed for such nanoparticles and is attributed to an increase of the size factor of the GNP.^{1,21} To avoid simultaneous excitation of the LSPR and the QDs, we choose CdTe QDs for their large Stoke shift between absorption and emission.^{16,22}

Typical photoluminescence spectra measured on different nanostructures containing CdTe quantum dots (with and without GNP arrays) are presented in Figure 2a. Each spectrum has been adjusted using a Gaussian profile.

First of all, we can observe that the photoluminescence (PL) maximum wavelength does not shift with the GNP diameter indicating that the band structure of the QDs is not affected by the GNPs and that there is no self-quenching by nonradiative energy transfer between QDs.²³ To study precisely the influence of GNPs on the QD photoluminescence, the intensity of the signal measured on the GNPs is normalized by the intensity of the signal measured on the bare sample (*i.e.*, an area in the QD/PMMA film without GNPs). Then, we obtained the PL modification factor F given by $F = S_m/S$, where S_m is the measured signal with the presence of GNPs and S is the measured signal without any GNPs.

The obtained modification factor of photoluminescence F is presented in Figure 2b as a function of the diameter of the considered GNPs. The photoluminescence from patterned areas exhibits both quenching and enhancement compared to that of unpatterned areas. For particle diameter below 120 nm, we observe a reduced PL compared to the intensity without the presence of GNP. At 130 nm diameter, the PL intensity equals that of the intensity without GNP. Only for a diameter >140 nm, is the PL intensity enhanced compared to the reference situation. Furthermore, the measured photoluminescence enhancement reaches 260% for the 160 nm diameter GNPs. To determine how the LSPR is correlated with the modification of the PL, we represent the modification factor F as a function of the difference between the wavelength of the measured LSPR (corresponding to the peak maximum measured by extinction spectroscopy in far field in PMMA/QD) and the wavelength of the QD emission (*i.e.*, $\Delta w = \lambda_{\text{LSPR}} - \lambda_{\text{QD}}$). The obtained results are shown Figure 2c. It clearly appears that the transition between the two limit behaviors (*i.e.*, quenching and exaltation of photoluminescence) is situated around $\Delta w = 40$ nm. This result means that the extinction maximum must be redshifted in respect of the QD photoluminescence wavelength to obtain $F > 1$. This shift corresponds to the shift between the absorption and the extinction spectra of GNPs as previously reported by several authors.^{24,25} We therefore infer that the GNPs absorb the light from the QD and then emit it. To check this assumption, we tune the distance between the GNPs and the QDs for many GNP sizes. Using an organic spacer (see Materials and Methods), we increased the GNP–QD interdistance from 3 nm to 13.5 nm with a step of about 1.5 nm. Measured spectra for different GNP–QD interdistances are presented Figure 3a for GNP of 80 nm ($F < 1$) and Figure 3b for GNP of 160 nm ($F > 1$), respectively. In the case of the smaller particles (*i.e.*, 80 nm), the PL signal increases with the interdistance. On the other hand, for the larger ones, the PL signal decreases with the thickness of the spacer. The PL modification factor F is represented Figure 4a as a function of the interdistance for all the samples.

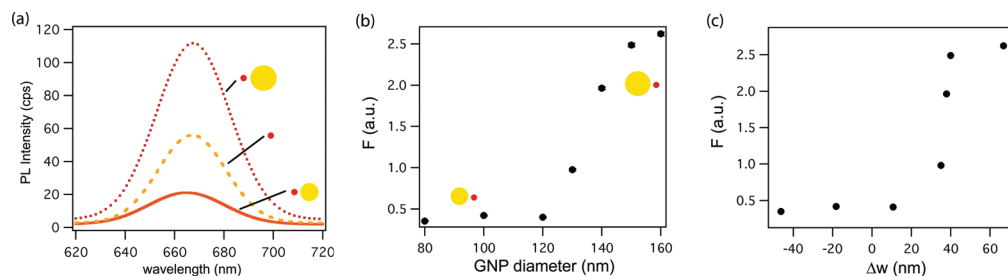


Figure 2. (a) Photoluminescence spectrum measured in the vicinity of GNP of 80 nm (line), without GNP (dash), and in the vicinity of GNP of 140 nm (dots), respectively. Note that the spectrum have been smoothed using a Gaussian fit. (b) Modification factor of photoluminescence F as a function of the diameter of the GNPs. (c) Modification factor of photoluminescence F as a function of $\Delta w = \lambda_{\text{LSPR}} - \lambda_{\text{QD}}$, the difference between the plasmon resonance wavelength and the QD emission wavelength.

F is strongly interdistance dependent except for the GNPs of 130 nm in diameter for which no variation is measured. For the small GNPs (diameter <130 nm) the quenching effect is reduced when the interdistance R is increased. For the largest GNPs (diameter >130 nm) the enhancement of luminescence diminishes with the increasing interdistance. In both cases, the modification of the PL completely disappears for an interdistance higher than 12 nm. This result suggests a strong distance dependent coupling between the GNPs and the QDs. Then, we represent the factor $E(R)$, corresponding to the coupling efficiency, as a function of the interdistance R (see Figure 4b), and given by

$$E(R) = \frac{|1 - F(R)|}{|1 - F_{\max}|} \quad (1)$$

where $F(R)$ is the F factor, function of the interdistance R , and F_{\max} is the maximum value of $F(R)$.

Assuming that both QD and GNP can be considered as dipoles,²⁶ the experimental data points are fitted using the function described by^{27,28}

$$E(R) = \sum_{n=2,3,4,6} \frac{C_n}{1 + \left(\frac{R}{R_n}\right)^n} \quad (2)$$

where C_n is a constant, R is the interdistance, and R_n is the interdistance corresponding to 50% of efficiency for the considered physical process whose nature depends on the integer n ($n = 2, 3, 4$, or 6). As clearly shown (Figure 4b) the experimental data points are well fitted using eq 2 with $n = 6$. The fit of the different curves shows that

$$E(R) \approx \frac{1}{1 + \left(\frac{R}{R_6}\right)^6}$$

with $R_6 \approx 7.5$ nm. This dependence corresponds to a nonradiative transfer between dipoles as evidenced by Förster.²⁸ Thus, our results clearly show that there is a nonradiative transfer (such as FRET) from the QDs to the GNPs.²⁷

In our experiments, the excitation wavelength is 405 nm. We emphasize that no plasmon mode of the GNPs is directly excited due to the fact that this excitation wavelength is far from the measured LSPR as clearly shown Figure 1. Thus, the photoluminescence enhancement cannot be explained by a local increase of the incident field intensity due to the LSPR. This would be characterized by an exponential decay of the F factor with the interdistance.¹⁰ At this wavelength, the absorption cross section σ_{abs} of the GNPs is higher than the scattering cross section σ_{scat} ²⁴ as shown in Figure 5a. The cross sections were obtained using Mie theory. The calculated dependence of the modification of the incident field ($N_{\text{ex}}\big|_{405} = \sigma_{\text{scat}}/\sigma_{\text{abs}}$) as a function of

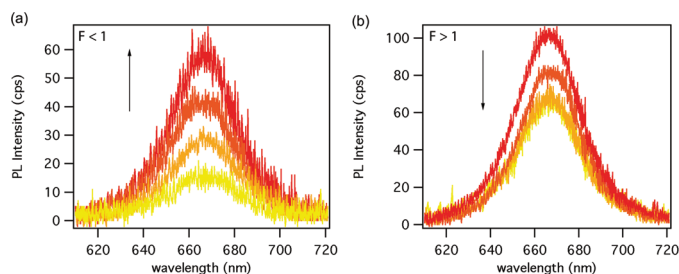


Figure 3. Measured spectra for different GNP–QD interdistances are presented (a) for GNP of 80 nm and (b) for GNP of 160 nm, respectively. Black arrows indicate the increasing distance QD–GNP.

the GNP diameter is shown in Figure 5b. ($N_{\text{ex}}\big|_{405} < 1$ for all the GNP sizes thus inducing a decrease of the local incident excitation field. The variation of N_{ex} tends to significantly reduce the quenching induced by the smallest GNPs (80 nm and 100 nm) and slightly increase the exaltation induced by the biggest ones. Nevertheless, the general behavior shown in Figure 2b is not significantly modified. Moreover, the incident intensity used ($\sim 120 \text{ W} \cdot \text{cm}^{-2}$) is too weak to induce a modification of the absorption cross section of the QDs. Contrarily to the experimental configuration used by Wang *et al.*,¹³ there is no TM component of the incident field thus avoiding an excitation of the out of plane plasmon. Besides, below 500 nm plasmon resonances are strongly damped by interband transitions.

The proposed process is schematically illustrated in Figure 6. The incident light absorbed by the GNPs at 405 nm induces interband transitions situated around 500 nm in gold.²⁹ This interband absorption induces an excited state (d-band holes with sp-band electrons) of the gold nanoparticles.

Then, depending on the GNP size, two scenarios are envisaged: first, for the smallest GNPs (diameter < 130 nm), all the transferred energy from the QDs is dissipated by Joule effect (*i.e.*, the electron–phonon coupling) because the plasmon state is off resonance with the PL of QDs and the measured signal at this wavelength is strongly reduced (see Figure 6a). On the other hand, for the larger GNPs (diameter >130 nm), the plasmon state is excited by the energy transferred from the QDs, thus allowing a new radiative way for the en-

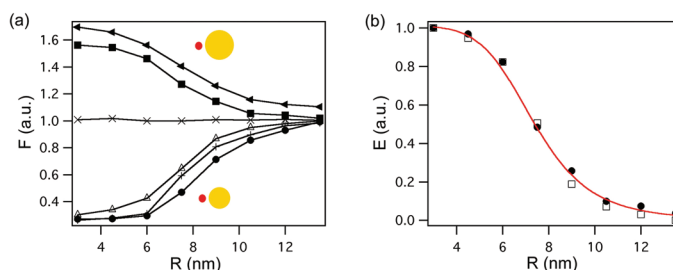


Figure 4. (a) Modification factor of photoluminescence F as a function of the interdistance between GNP and the QDs for a diameter of GNP of about 80 (black circle), 100 (+), 120 (triangle up), 130 (x), 140 (black square), and 160 nm (black triangle left). (b) Coupling efficiency E as a function of the interdistance R for a diameter of GNP of about 80 (black circle) and 140 nm (square). Red line is a fit obtained using eq 2.

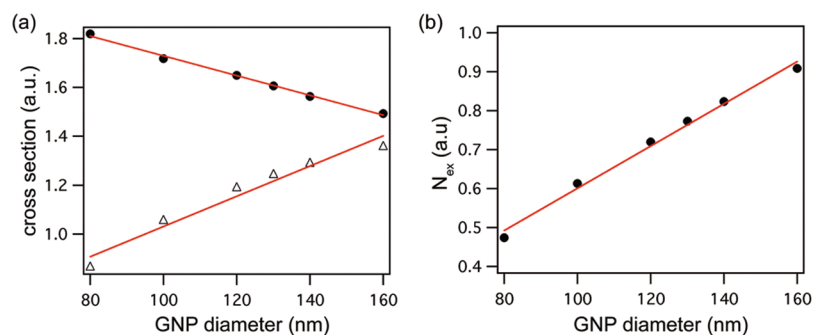


Figure 5. (a) Calculated (\bullet) absorption cross section σ_{abs} and (Δ) scattering cross section σ_{scat} of the GNPs for all the sizes at 405 nm. (b) Calculated dependence of the modification of the local field $(N_{\text{ex}})_{405} = \sigma_{\text{scat}}/\sigma_{\text{abs}}$ as a function of the GNP diameter.

ergy dissipation (see Figure 6b, relaxation way (8)). In that case, the electron–hole pairs will recombine by emitting a radiative plasmon³⁰ at the same frequency in a process similar to stimulated emission of plasmon state. The plasmon is excited by the QD PL transferred energy and the very short lifetime of the plasmon state ($\ll 100$ fs)³¹ does not induce a measurable modification of the spectrum at room temperature (*i.e.*, no noticeable shift or damping of the QD photoluminescence has been measured at 665 nm). It simply induces a strong enhancement of the measured signal at the same apparent wavelength as schematized Figure 6b. Note that the difference in intensity of the measured signal between the different GNP comes from the different probabilities of radiative emission of the considered plasmon state. Then, the new emitter system composed by a GNP strongly coupled with several QDs exhibits a higher brightness than a bare QD in the case of the largest GNPs.

CONCLUSION

To summarize, we showed the possibility of tuning under control the emission efficiency of hybrid semiconductor-metal nanosource for a large range of gold nanoparticle sizes. We show that the modification factor of emission of hybrid nanosource compared with bare quantum dots depends strongly on the GNP size (*i.e.*, plasmon resonance). Moreover, our results clearly show a strong nonradiative energy transfer from semiconductor quantum dots to gold nanoparticles. Particularly, we show that the distance dependence of this energy transfer fits perfectly with a dipole–dipole coupling. Our observations can be explained by the creation of particle plasmon through interband absorption which emits photons when excited by the energy transferred from the quantum dots. These results bring crucial knowledge to develop bright and localized nanosources required in future nanophotonic devices.

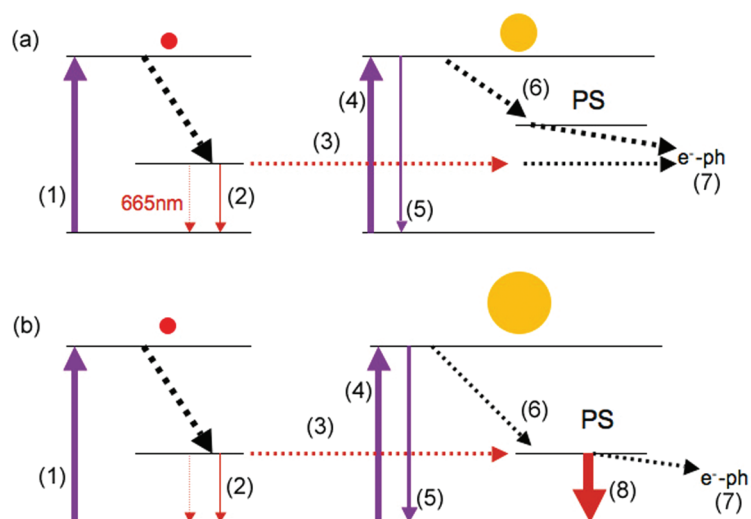


Figure 6. Simplified representation of the physical process (a) in the case of GNPs with a diameter <130 nm and (b) in case of GNPs with a diameter >130 nm. The different steps are (1) absorption of the incident laser beam by the QD, (2) emission process of the QD, (3) energy transferred nonradiatively from the QD to the GNP, (4) interband absorption of the incident laser beam by the GNP, (5) scattering of the incident laser beam, (6) nonradiative intraband transitions, (7) thermal deexcitation by electron–phonon coupling, and (8) radiative deexcitation from the plasmon state (PS).

MATERIALS AND METHODS

Preparation of the Samples. Gold nanoparticles were fabricated by electron beam lithography technique and lift off offering thus the possibility to control precisely size, shape, and interdistance of metal nanostructures.³² The GNP diameters vary from 80 to 160 nm and the height is 50 nm. The interdistance is kept constant at 200 nm to avoid near field coupling between GNP. The quantum dots used are core-shell CdTe/CdS (Evident Technologies) with 665 nm emission wavelength and a quantum yield of about 30–40% in toluene. The total diameter of QDs is about 8–9 nm, and the core diameter is about 3–4 nm. The QDs are diluted in toluene (90 $\mu\text{g}/\text{nmol}$) and added to the PMMA solution (3 g/L). Quantum-dot-doped PMMA thin film is then spin-coated on the metal nanoparticles at 3000 rpm. The thickness of the obtained film is 10 ± 1.5 nm, as determined by AFM measurements. Thus, a quasi-monolayer of quantum dots above the GNP arrays is obtained. The QD-GNP distance is controlled through a layer-by-layer deposition of polyelectrolytes. Polyelectrolyte multilayers were deposited by alternate dipping of the substrate in aqueous solutions (pH = 3, 10 mM in monomer unit, without salts) of PDDA (poly(diallyldimethylammonium chloride), $M_w = 100\,000$ to 200 000) and PSS (poly(styrenesulfonate), $M_w = 70\,000$).^{33,34}

Optical Characterizations. Visible extinction spectra were measured using a micro-Raman spectrometer (Labram, Jobin Yvon) in standard transmission geometry with unpolarized white light. The transmitted light is collected with a 10 \times objective (N.A. = 0.25) from an area of $30 \times 30 \mu\text{m}^2$. The extinction spectra were used to determine the position of the localized surface plasmon resonance of bare and hybrid nanostructures (*i.e.*, after the composite QD/PMMA deposition). To study the photoluminescence, quantum dots are excited through a polymer microlens localized at the extremity of a monomode fiber.³⁵ The distance in the near field region between the microlens and the sample is controlled by a shear force set up.³⁵ The excitation wavelength is 405 nm. The luminescence is collected at 45 $^\circ$ in far field through a long working distance objective (50 \times , 0.42 N.A.) and directed on a spectrophotometer in order to measure quantum dot luminescence spectrum.

Acknowledgment. We are grateful to R. Bachelot, A. Bouhelier, and D. Gerard for fruitful discussions. This work was financed by ANR (2007 “photohybrid”) and the Région Champagne-Ardenne (Projet Émergence E2007-08052).

REFERENCES AND NOTES

- Maier, S. *Plasmonics: Fundamentals and Applications*; Springer: New York, 2007.
- Pelton, M.; Aizpurua, J.; Bryant, G. Metal–Nanoparticle Plasmonics. *Laser Photonics Rev.* **2008**, *2*, 136–159.
- ibn el Ahrach, H.; Bachelot, R.; Vial, A.; Lerondel, G.; Plain, J.; Royer, P.; Soppera, O. Spectral Degeneracy Breaking of the Plasmon Resonance of Single Metal Nanoparticles by Nanoscale Near-Field Photopolymerization. *Phys. Rev. Lett.* **2007**, *98*, 107402.
- Schatz, G. C.; Young, M.; Duynes, R. P. V. Electromagnetic Mechanism of SERS. *Top. Appl. Phys.* **2006**, *103*, 19–46.
- Lakowicz, J.; Fu, Y. Modification of Single Molecule Fluorescence Near Metallic Nanostructures. *Laser Photonics Rev.* **2009**, *3*, 221–232.
- Bergman, D.; Stockman, M. Surface Plasmon Amplification by Stimulated Emission of Radiation: Quantum Generation of Coherent Surface Plasmons in Nanosystems. *Phys. Rev. Lett.* **2003**, *90*, 027402.
- Stockman, M. I. Spasers Explained. *Nat. Photonics* **2008**, *2*, 327–329.
- Noginov, M. A.; Zhu, G.; Belgrave, A. M.; Bakker, R.; Shalaev, V. M.; Narimanov, E. E.; Stout, S.; Herz, E.; Suteewong, T.; Wiesner, U. Demonstration of a Spaser-Based Nanolaser. *Nature* **2009**, *460*, 1110–1112.
- Dulkeith, E.; Morteaux, A.; Niedereichholz, T.; Klar, T.; Feldmann, J.; Levi, S.; van Veggel, F.; Reinhoudt, D.; Moller, M.; Gittins, D. Fluorescence Quenching of Dye Molecules Near Gold Nanoparticles: Radiative and Nonradiative Effects. *Phys. Rev. Lett.* **2002**, *89*, 203002.
- Anger, P.; Bharadwaj, P.; Novotny, L. Enhancement and Quenching of Single-Molecule Fluorescence. *Phys. Rev. Lett.* **2006**, *96*, 113002.
- Tam, F.; Goodrich, G. P.; Johnson, B. R.; Halas, N. J. Plasmonic Enhancement of Molecular Fluorescence. *Nano Lett.* **2007**, *7*, 496–501.
- Kuehn, S.; Hakanson, U.; Rogobete, L.; Sandoghdar, V. Enhancement of Single-Molecule Fluorescence Using a Gold Nanoparticle as an Optical Nanoantenna. *Phys. Rev. Lett.* **2006**, *97*, 017402.
- Wang, Y.; Yang, T.; Tuominen, M. T.; Achermann, M. Radiative Rate Enhancements in Ensembles of Hybrid Metal–Semiconductor Nanostructures. *Phys. Rev. Lett.* **2009**, *102*, 163001.
- Gueroui, Z.; Libchaber, A. Single-Molecule Measurements of Gold-Quenched Quantum Dots. *Phys. Rev. Lett.* **2004**, *93*, 166108.
- Kulakovich, O.; Strelak, N.; Yaroshevich, A.; Maskevich, S.; Gaponenko, S.; Nabiev, I.; Woggon, U.; Artemyev, M. Enhanced Luminescence of CdSe Quantum Dots on Gold Colloids. *Nano Lett.* **2002**, *2*, 1449–1452.
- Pompa, P.; Martiradonna, L.; Della Torre, A.; Della Sala, F.; Manna, L.; De Vittorio, M.; Calabi, F.; Cingolani, R.; Rinaldi, R. Metal-Enhanced Fluorescence of Colloidal Nanocrystals with Nanoscale Control. *Nat. Nanotechnol.* **2006**, *1*, 126–130.
- Song, J.; Atay, T.; Shi, S.; Urabe, H.; Nurmikko, A. Large Enhancement of Fluorescence Efficiency from CdSe/ZnS Quantum Dots Induced by Resonant Coupling to Spatially Controlled Surface Plasmons. *Nano Lett.* **2005**, *5*, 1557–1561.
- Tovmachenko, O.; Graf, C.; van den Heuvel, D.; van Blaaderen, A.; Gerritsen, H. Fluorescence Enhancement by Metal-Core/Silica-Shell Nanoparticles. *Adv. Mater.* **2006**, *18*, 91–95.
- Shimizu, K.; Woo, W.; Fisher, B.; Eisler, H.; Bawendi, M. Surface-Enhanced Emission from Single Semiconductor Nanocrystals. *Phys. Rev. Lett.* **2002**, *89*, 117401.
- Chen, Y.; Munechika, K.; Ginger, D. Dependence of Fluorescence Intensity on the Spectral Overlap Between Fluorophores and Plasmon Resonant Single Silver Nanoparticles. *Nano Lett.* **2007**, *7*, 690.
- Bouhelier, A.; Bachelot, R.; Im, J.; Wiederrecht, G.; Lerondel, G.; Kostcheev, S.; Royer, P. Electromagnetic Interactions in Plasmonic Nanoparticle Arrays. *J. Phys. Chem. B* **2005**, *109*, 3195–3198.
- Chen, Y.; Munechika, K.; Plante, I. J.-L.; Munro, A.; Skrabalak, S.; Xia, Y.; Ginger, D. Excitation Enhancement of CdSe Quantum Dots by Single Metal Nanoparticles. *Appl. Phys. Lett.* **2009**, *93*, 053106.
- Plain, J.; Sonnefraud, Y.; Viste, P.; Lerondel, G.; Huang, S.; Royer, P. Self-Assembly Drives Quantum Dot Photoluminescence. *J. Fluoresc.* **2009**, *19*, 311–316.
- Messinger, B.; von Raben, K. U.; Chang, R.; Barber, P. Local Fields at the Surface of Noble-Metal Microspheres. *Phys. Rev. B* **1981**, *24*, 649–657.
- Ross, B.; Lee, L. Comparison of Near- and Far-Field Measures for Plasmon Resonance of Metallic Nanoparticles. *Opt. Lett.* **2009**, *34*, 896–898.
- Liu, G. L.; Long, Y. T.; Choi, Y.; Kang, T.; Lee, L. P. Quantized Plasmon Quenching Dips Nanospectroscopy via Plasmon Resonance Energy Transfer. *Nat. Methods* **2007**, *4*, 1015–1018.
- Carminati, R.; Greffet, J.; Henkel, C.; Vigoureux, J. Radiative and Non-Radiative Decay of a Single Molecule Close to a Metallic Nanoparticle. *Opt. Commun.* **2006**, *261*, 368–375.
- Förster, T. 10th Spiers Memorial Lecture. Transfer Mechanisms of Electronic Excitation. *Discuss. Faraday Soc.* **1959**, *27*, 7–17.
- Mooradian, A. Photoluminescence of Metals. *Phys. Rev. Lett.* **1969**, *22*, 185–187.

30. Dulkeith, E.; Niedereichholz, T.; Klar, T.; Feldmann, J.; von Plessen, G.; Gittins, D.; Mayya, K.; Caruso, F. Plasmon Emission in Photoexcited Gold Nanoparticles. *Phys. Rev. B* **2004**, *70*, 205424.
31. Sönnichsen, C.; Franzl, T.; Wilk, T.; Plessen, G. V.; Feldmann, J.; Wilson, O.; Mulvaney, P. Drastic Reduction of Plasmon Damping in Gold Nanorods. *Phys. Rev. Lett.* **2002**, *88*, 774021–774024.
32. Grand, J.; Kostcheev, S.; Bijeon, J.; de la Chapelle, M.; Adam, P.; Romyantseva, A.; Lerondel, G.; Royer, P. Optimization of SERS-Active Substrates for Near-Field Raman Spectroscopy. *Synth. Met.* **2003**, *139*, 621–624.
33. Decher, G. Fuzzy Nanoassemblies: Toward Layered Polymeric Multicomposites. *Science* **1997**, *277*, 1232–1237.
34. Barbillon, G.; Bijeon, J.-L.; Plain, J.; de la Chapelle, M. L.; Adam, P.-M.; Royer, P. Biological and Chemical Gold Nanosensors Based on Localized Surface Plasmon Resonance. *Gold Bull.* **2007**, *40*, 240–244.
35. Juan, M.; Bouillard, J. S.; Plain, J.; Lerondel, G.; Adam, P. M.; Bachelot, R.; Royer, P. Near-Field Investigation of Porous Silicon Photoluminescence Modification after Oxidation in Water. *J. Microsc. (Oxford, U.K.)* **2008**, *229*, 469–474.